



Evaluation of the potential of MODIS satellite data to predict vegetation phenology in different biomes: An investigation using ground-based NDVI measurements

G. Hmimina^a, E. Dufrêne^a, J.-Y. Pontailler^a, N. Delpierre^a, M. Aubinet^b, B. Caquet^d, A. de Grandcourt^d, B. Burban^e, C. Flechard^f, A. Granier^c, P. Gross^c, B. Heinesch^b, B. Longdoz^c, C. Moureaux^b, J.-M. Ourcival^g, S. Rambal^g, L. Saint André^h, K. Soudani^{a,*}

^a University of Paris-Sud, CNRS, AgroParisTech, Laboratoire Ecologie Systematique et Evolution, Faculty of Sciences of Orsay, France

^b University of Liège – Gembloux Agro-Bio Tech (GxABT), Passage des Déportés 2, Gembloux, Belgium

^c INRA, UMR EEF 1137, INRA/University of Nancy, Champenoux, France

^d CIRAD/CRDPI, France

^e INRA, UMR Ecofog, Kourou, Guyane Française, French Guiana

^f INRA, Agrocampus Ouest, UMR 1069 SAS, Rennes, France

^g CNRS, Centre d'Ecologie Fonctionnelle et Evolutive, Montpellier, France

^h INRA, Unité Biogéochimie des Ecosystèmes Forestiers, Champenoux, France

ARTICLE INFO

Article history:

Received 5 June 2012

Received in revised form 17 December 2012

Accepted 12 January 2013

Available online 11 February 2013

Keywords:

Ground-based NDVI

MODIS

Deciduous forests

Evergreen forests

Crops

Phenology

ABSTRACT

Vegetation phenology is the study of the timing of seasonal events that are considered to be the result of adaptive responses to climate variations on short and long time scales. In the field of remote sensing of vegetation phenology, phenological metrics are derived from time series of optical data. For that purpose, considerable effort has been specifically focused on developing noise reduction and cloud-contaminated data removal techniques to improve the quality of remotely-sensed time series. Comparative studies between time series composed of satellite data acquired under clear and cloudy conditions and from radiometric data obtained with high accuracy from ground-based measurements constitute a direct and effective way to assess the operational use and limitations of remote sensing for predicting the main plant phenological events. In the present paper, we sought to explicitly evaluate the potential use of MODerate resolution Imaging Spectroradiometer (MODIS) remote sensing data for monitoring the seasonal dynamics of different types of vegetation cover that are representative of the major terrestrial biomes, including temperate deciduous forests, evergreen forests, African savannah, and crops. After cloud screening and filtering, we compared the temporal patterns and phenological metrics derived from in situ NDVI time series and from MODIS daily and 16-composite products. We also evaluated the effects of residual noise and the influence of data gaps in MODIS NDVI time series on the identification of the most relevant metrics for vegetation phenology monitoring. The results show that the inflexion points of a model fitted to a MODIS NDVI time series allow accurate estimates of the onset of greenness in the spring and the onset of yellowing in the autumn in deciduous forests (RMSE \leq one week). Phenological metrics identical to those provided with the MODIS Global Vegetation Phenology product (MDC12Q2) are less robust to data gaps, and they can be subject to large biases of approximately two weeks or more during the autumn phenological transitions. In the evergreen forests, in situ NDVI time series describe the phenology with high fidelity despite small temporal changes in the canopy foliage. However, MODIS is unable to provide consistent phenological patterns. In crops and savannah, MODIS NDVI time series reproduce the general temporal patterns of phenology, but significant discrepancies appear between MODIS and ground-based NDVI time series during very localized periods of time depending on the weather conditions and spatial heterogeneity within the MODIS pixel. In the rainforest, the temporal pattern exhibited by a MODIS 16-day composite NDVI time series is more likely due to a pattern of noise in the NDVI data structure according to both rainy and dry seasons rather than to phenological changes. More investigations are needed, but in all cases, this result leads us to conclude that MODIS time series in tropical rainforests should be interpreted with great caution.

© 2013 Elsevier Inc. All rights reserved.

1. Introduction

Vegetation phenology is the study of the timing of seasonal events, such as leaf budburst and leaf senescence, that are considered to be the result of adaptive responses to climatic constraints. As such, an understanding of phenology brings important insights into both climate and

* Corresponding author. Tel.: +33 1 69 15 64 27.

E-mail address: kamel.soudani@u-psud.fr (K. Soudani).

vegetation interactions and their impacts on matter and energy exchange processes at local, regional and global scales. Because field phenological observations are work intensive and cannot be easily generalized, remote-sensing tools were developed to track Earth surface changes. The use of satellite-derived vegetation indices is now frequent in the literature and has been closely linked to canopy foliage biomass (Soudani et al., 2006), the onset of leaf greenness in the spring and the onset of leaf coloring in the autumn (Soudani et al., 2008; Zhang & Goldberg, 2011; Zhang et al., 2003). Remote sensing-based phenology began with the Advanced Very High Resolution Radiometer (AVHRR) (Reed et al., 1994) and has been significantly improved with the Moderate Resolution Imaging Spectroradiometer (MODIS) onboard Terra and Aqua satellites (Zhang et al., 2003). Data are acquired daily by AVHRR and MODIS sensors, but MODIS represents a significant improvement in terms of spatial resolution (250 m to 1 km vs. 1 km), spectral resolution (36 spectral bands vs. 6), geolocation accuracy [50 m at nadir (Wolfe et al., 2002) vs. 1 to 2 km (Box et al., 2006)], the atmospheric correction scheme and cloud screening (Heidinger et al., 2001) and sensor calibration (Justice et al., 1998). MODIS data are now used routinely for building the MODIS global vegetation phenology product that provides estimates of the timing of main vegetation seasonal cycles events at global scales. The first version of this product (MOD12Q2) was already evaluated, particularly in the studies of Zhang et al. (2003) and Soudani et al. (2008). Since 2009, a new version of the global vegetation phenology product (MCD12Q2) has been available that covers the period from 2001 through 2006. Compared to the first version, MCD12Q2 uses MODIS with both Aqua and Terra platforms at higher spatial and temporal resolutions (500 m vs. 1 km and 8 days vs. 16 days). The first validation studies of this product are underway (Ganguly et al., 2010).

In the field of remote vegetation phenology sensing, considerable effort has been focused on developing noise reduction and cloud-contaminated data removal techniques [e.g., Best Index Slope Extraction (BISE) (Viovy et al., 1992), a CVA-MVC compositing algorithm used to produce MODIS-based global vegetation phenology products (Huete et al., 2002), an adaptive Savitzky–Golay filter (Chen et al., 2004) and a mean value iteration filter (Ma & Veroustraete, 2006)]. Different phenological markers were then derived from remotely-sensed time series data after filtering and noise reduction pre-processing. These phenological markers may be categorized as follows (Soudani et al., 2008): (1) user-defined thresholds separating growing and dormancy seasons (Chen et al., 2004; Delbart et al., 2006; Schwartz et al., 2002; Studer et al., 2007; Suzuki et al., 2003; White & Nemani, 2006; White et al., 1997, 2002); (2) markers based on significant and rapid increases in remotely-sensed signals (Kaduk & Heimann, 1996; Moulin et al., 1997; Schwartz et al., 2002) and (3) parameters directly determined from functions fitted to remotely-sensed time series data (Beck et al., 2006; Fisher et al., 2006; Jönsson & Eklundh, 2002; Soudani et al., 2008; Zhang et al., 2003). These phenological markers are related to the vegetation cover types characterized by strong and rapid changes in leaf density that are sufficient to be detected by remote sensing sensors. These phenological markers focus on the beginning and end of the vegetation season, that is, the beginning and end of the period of canopy photosynthesis, respectively. These events are characteristic of the phenology of deciduous species. The timing of the beginning of the photosynthetically active period is associated with the emergence of buds and the first leaves. The timing of the end of this period is characterized by depigmentation, leaf yellowing and then leaf fall under the control of abscission processes. For evergreen species that show less seasonal change in foliage biomass, the noise inherent to satellite-based radiance measurements may completely mask the seasonal variations (Moulin et al., 1997). This interference may explain the fact that few studies have been devoted to the evergreen vegetation and that the potential use of remote sensing to monitor the seasonal dynamic of these biomes has not been sufficiently assessed.

Despite the technological maturity and significant progress achieved over the last 10 years, there remains a strong need for an effective and

unbiased assessment of the potential and practical use of remotely-sensed data to monitor vegetation phenology. Indeed, the consequences of applying pre-processing techniques (atmospheric corrections, noise filtering, and compositing methods) on the performance of remotely-sensed time series for detecting phenological events have been evaluated under specific conditions through limited comparisons of one method against others without referring to field observations (Chen et al., 2004) or through comparisons with field observations that are themselves subject to multiple sources of uncertainty (operator bias, sampling density, temporal frequency, data compilation process, etc.). However, the multitude of remote sensing-based phenological metrics used can also make an accurate evaluation of the applicability of remote sensing for the detection of key vegetation phenological events much more difficult (White et al., 2009). Finally, from a practical point of view, phenological metrics provide many estimates that correspond to different phenological situations, making their practical use in other studies problematic. Therefore, comparative studies between time series composed of satellite data in clear and cloudy conditions and of high-accuracy radiometric data obtained from ground-based measurements constitute a direct and effective way to assess the operational use and limitations of remote sensing in predicting the main plant phenological events. In this study, we sought to explicitly evaluate the potential use of MODIS remote sensing data for monitoring the seasonal dynamics of vegetation cover from in situ NDVI measurements in different vegetation cover types that are representative of the major terrestrial biomes, including temperate deciduous forests of oak and beech, an evergreen forest, a tropical rainforest, an African savannah, and a succession of crops. This assessment relies on tower-based measurements of NDVI at a half-hourly time step. After cloud screening and filtering, we will 1) compare temporal patterns and phenological metrics derived from in situ NDVI time series and from a MODIS daily and 16-day composite product and 2) evaluate the effects of residual noise and the influence of data gaps in the MODIS NDVI time series to identify the most relevant metrics for vegetation phenology monitoring.

2. Materials and methods

2.1. Study sites

This study was undertaken at seven experimental sites that are members of FLUXNET, the global network of eddy covariance flux towers measuring carbon, water and energy fluxes between the vegetation and atmosphere. These study sites cover three main bioclimatic regions (temperate, Mediterranean, and tropical) and the major plant functional types encountered: deciduous and evergreen forests, tropical moist evergreen forest, African savannah, and crops (Table 1). More details about these sites are provided in Soudani et al. (2012).

Briefly, the temperate deciduous forests are situated in the Fontainebleau, Hesse, and Fougères regions in the Northern France. The two main overstorey species are: sessile and pedunculate Oaks [*Quercus petraea* (Matt.) Liebl and *Quercus robur* L.] in the Fontainebleau forest, and beech (*Fagus sylvatica* L.) in the Hesse and Fougères forests. The Hesse site is described in more details in Granier et al. (2008).

The evergreen forests are situated in the Puechabon region in Southern France. The Puechabon site is a holm oak (*Quercus ilex* L.) evergreen broadleaf forest. It is located on the northern Mediterranean coast, and is representative of the whole region. Holm oak is emblematic of Mediterranean sclerophyllous vegetation and is encountered in Southern Europe and the Arab Maghreb region in Northern Africa.

The tropical rainforest site is located in Paracou in French Guiana (Guyflux experimental site). It is a mature forest with unknown human disturbance over the past centuries. This forest is characterized by a high diversity of plant species. The major species are in the families of *Caesalpinaceae*, *Lecythidaceae*, *Chrysobalanaceae*, and *Sapotaceae*. More details about this experimental site are provided in Bonal et al. (2008).

The African savannah is located in the Tchizalamou study site (North–North-East of Pointe Noire – Congo). This site is part of the CARBOAFRICA network. It is composed of grassland dominated by the grass *Loudetia simplex* (Nees) Hubb., one of the most common species in this region of West Africa, with sparse shrubs of *Annona arenaria* (Schumacher & Thonn.). This area is burnt every year almost at the same date at the end of June. More details about this experimental site are provided in Castaldi et al. (2010).

The succession of crops is located in Lonzee in the Belgian province of Namur. It is composed of a succession of annual crops over three years at the same location as wheat (2007), sugar beet (2008), and wheat and mustard (2009). This site is part of CarboEurope-IP, and more details about this site and the farming operations are provided in Aubinet et al. (2009) and Dufranne et al. (2011).

For each site except the Guyaflux site, spatial representativity of the main species present in the MODIS pixel and “seen” by the in situ sensor is shown in Table 1. It is calculated as the ratio of basal areas (or biomass in Tchizalamou site) of species present in the field of view of in situ sensor to total basal area within MODIS pixel from field inventories. In forest stands field inventories were done on the whole MODIS pixel in Hesse and Fontainebleau sites (for Hesse forest, more details are given in Granier et al. (2008) and for Fontainebleau forest, data are unpublished but details about the forest stand are given in Delpierre et al. (2009)). In Fougere forest, field inventories were done in December 2010 on an area of approximately 10,000 m² surrounding the flux tower. Both in and outside the sampled area, over the MODIS pixel, the stand is almost monospecific, composed of beech (unpublished data). In the Puechabon forest, inventory was made on 12 plots of 100 m² each around the tower. As shown in Table 1, the holm oak occupies about 96% of total basal area (31 m²/ha versus 32.3 m²/ha). This composition is considered as homogeneous on the 50 ha of the forest management unit and beyond, because the management over the past century was exactly the same across the whole forest region as shown in Goerner et al. (2009). In the tropical rainforest, as underlined above, there is a high specific diversity, including up to 180 different trees/ha, but no species is dominant. In the grassland savanna, *Loudetia simplex*, followed by *Ctenium newtonii* Hack. (Poaceae) accounted for more than 75% of the aerial total phytomass regardless of the season. The Lonzee herbaceous site, as shown in Dufranne et al. (2011), is a homogeneous agricultural area of about 12 ha.

2.2. In situ NDVI measurements and pre-processing

In situ measurements of NDVI were achieved using a laboratory-made sensor. More details about this NDVI sensor and the in situ measurement protocol are provided in Soudani et al. (2012). Briefly, NDVI sensors are made according to the design described in Pontailleur et al. (2003) and Pontailleur and Genty (1996). The body of the sensor is made of Teflon® installed into a stainless steel cylinder having a diameter of 3 cm and a height of 9 cm and is equipped with two photodiodes having spectral sensitivity in red and near-infrared bands. The two photodiodes are covered with two filters resulting in bandwidths of 640–660 nm and 780–920 nm for red and near infrared, respectively. The technical specifications of the components of the sensor are provided in Soudani et al. (2012). The sensor was calibrated against a spectroradiometer (LI-1800, LI-COR, Inc.). NDVI sensors are installed on towers above the vegetation, directed downward at a height of several meters above the top of the canopy. The sensor is inclined at approximately 30° from the vertical and oriented towards the south to avoid a hotspot effect. The field of view is 100°, but it is often collimated to account for viewing constraints encountered at each site. The area viewed is approximately tens to hundreds of square meters, depending on the site. The data were recorded at half-hour time steps in a data-storage central unit. The NDVI is computed for measured radiances reflected by the canopy.

The processing of in situ measurements of NDVI was achieved according to Soudani et al. (2012). Only daily radiance measurements acquired under clear sky conditions during the time of the MODIS overpass are considered in this study.

2.3. MODIS NDVI data and pre-processing

For this study, we used two MODIS products: MODIS NDVI MOD13Q1 V005 16-day composites and MOD09GQK daily surface reflectance at a 250 m resolution. The MOD13Q1 V005 16-day 250 m NDVI for years 2000 to 2009 were obtained through the MODIS Subset gateway for the pixels centered on the study sites. The MOD13Q1 NDVI values were built using the Constrained View Angle Maximum Value Composite (CV-AMVC) algorithm on a 16-day compositing period described in Huete et al. (2002). The day of the year for each retained NDVI value is provided. The MODIS/TERRA surface reflectance daily L2G global 250 m V005 product (MOD09GQK) was obtained through the Earth Observing

Table 1

Main characteristics of the study sites. Percent coverage quantifies the spatial representativity of the species “seen” by the in situ sensor over the MODIS pixel. This representativity is calculated on the basis of basal areas (or biomass in savanna) of the species present in the MODIS pixel from field inventories.

Site name	Type of biome	Lat/long	Altitude (m)	Average temperature (°C)	Average precipitation (mm)	Main vegetation species	Age (years)	Maximum Leaf Area Index (m ² /m ²)	Percent coverage of main species
Fontainebleau	Deciduous broadleaf	48°28'35" N 2°46'48" E	120	10.2	720	Sessile and pedunculate Oaks (<i>Quercus petraea</i> (Matt.) Liebl and <i>Quercus robur</i> L.)	145	5	80%
Hesse	Deciduous broadleaf	48°40'27" N 7°03'56" E	300	9.2	820	European beech (<i>Fagus sylvatica</i> L.)	44	5.6	95%
Fougères	Deciduous broadleaf	48°22'59" N 1°11'05" W	140	11.2	900	European beech	40	–	95%
Puechabon	Evergreen broadleaf forest	43°44'29" N 3°35'45" E	270	13.4	907	Holm Oak (<i>Quercus ilex</i> L.)	70	2.9	96%
French Guiana	Tropical rain forest	5°16'54" N 52°54'44" W	29	25.7	3136	150 species (DBH > 10 cm)/ha	–	7	–
Tchizalamou (Congo)	Herbaceous Savanna	4°17'210" S 11°39'23" E	82	25.7	1150	<i>Loudetia simplex</i>	–	1.6	75%
Lonzee (Belgium)	Succession of crops	50° 33' 8" N 04° 44' 42" E	165	10	800	Succession Wheat/Sugar beet/Wheat and mustard	–	–	100%

System Data Gateway. We used the MODIS Reprojection Tool to extract the red and near-infrared bands and MODIS per-pixel quality assurance.

For each site, we used the pixel centered on the study site for each band and year, and we compiled them using MATLAB software (MATLAB 2008a, MathWorks, Natick, Massachusetts, USA). The NDVI was computed using MOD09GQK MODIS/Terra bands 1 (red: 630–690 nm) and 2 (near infrared: 780–900 nm) data produced at “ideal global quality”.

$$NDVI = \frac{NIR - RED}{NIR + RED} \quad (1)$$

Where *NIR* stands for the measured reflectance in the near infrared band and *RED* stands for the measured reflectance in the red band.

Unlike the MOD13Q1 products, which were already filtered using the 16-day CVA-MVC algorithm, daily MOD09GQK NDVI measurements are highly noisy despite the removal of pixels not flagged as “produced at ideal quality” in the pixel-level quality assurance (QA) image that provides QA descriptions about each pixel. Therefore, in this study, we developed the following scheme to improve the NDVI time series data. This scheme includes two steps:

- The removal of all values that can be considered unlikely considering what is known about the annual cycle of vegetation greenness using a Gaussian mixture model (GMM, McLachlan & Peel, 2000). For all studied biomes, we considered that the NDVI distribution is bimodal. The two modes correspond to low and high NDVI values. Low values coincide with the winter dormancy period in deciduous forests and periods of bare soils and low vegetation cover in crops and savannah. In evergreen forests, low NDVI values coincide with the short periods of leaf renewal that generally occur in the spring.
- The reduction of random noise using a moving-window mean filter based on the one described in Soudani et al. (2008).

First, to remove unlikely NDVI values contaminated by clouds and snow, a GMM was fitted on the distribution of NDVI values for each site and each year.

The two resulting Gaussian densities $N(\mu_1, \sigma_1)$ and $N(\mu_2, \sigma_2)$ with $\mu_1 < \mu_2$ provide three classes of NDVI values defined for each year, as follows:

- High NDVI values found in the $[\mu_2 - 2 * \sigma_2; \mu_2 + 2 * \sigma_2]$ interval.
- Intermediate values found in the $[\mu_1 + 2 * \sigma_1; \mu_2 - 2 * \sigma_2]$ interval.
- Low NDVI values found in the $[\mu_1 - 2 * \sigma_1; \mu_1 + 2 * \sigma_1]$ interval.

All NDVI values that were not within these bounds were discarded.

Second, we checked the distribution of NDVI acquisition dates in each of the three NDVI classes defined above. We assumed that the NDVI time series should exhibit coherent temporal patterns that predominate over noise and that most noisy observations correspond to low NDVI values. The few low NDVI observations occurring during periods that exhibit mostly high NDVI values are hereby considered as noise and vice versa. Formally, the NDVI filtering process was applied according to the following rules:

- High NDVI values acquired on the dates that were closer to the modal date of the low NDVI value class than to the modal date of the high NDVI value class were discarded and vice versa.
- Intermediate values acquired during the dates that fell in the period of the high NDVI class were discarded.
- Low NDVI values acquired during the dates that fell in the period of the intermediate NDVI class were discarded.

After this first step of processing, the retained NDVI values were filtered and smoothed according to the algorithm presented in Soudani et al. (2008) using an 11-day moving window and excluding NDVI values lower than the average value minus the standard deviation of the NDVI values within the moving window.

2.4. Deriving phenological metrics from NDVI time series

For deciduous canopies, an asymmetric double-sigmoid function (ADS) was fitted to the NDVI time series independently for each year using the following equation:

$$NDVI(t) = p * t + (a + c) + \frac{1}{2} * (a - c) * (\tanh(b * (t - \mu))) - \frac{1}{2} * (a - e) * \tanh(d * (t - v)) \quad (2)$$

\tanh is the hyperbolic tangent, t is the time (day of year) and $a, b, c, d, e, u, v,$ and p are the fitting parameters, where $(a + c)$ is the winter NDVI value and $(a - e)$ is the amplitude of the NDVI variation. u and v are the dates corresponding to the highest rates of change of $NDVI(t)$ (maximum and minimum peaks of the first derivative of $NDVI(t)$) (Fig. 1). They are the dates of the two inflexion points when $NDVI(t)$ increases during leaf expansion (u) and decreases during leaf senescence (v). u and v correspond to S_2 and A_2 shown in Fig. 1, respectively.

Note that Eq. (2) is based on the equation of Zhang et al. (2003), rewritten as in Soudani et al. (2008) but modified by including two new parameters (e and p). The additional parameter e allows Eq. (2) to fit two different winter NDVI minima for the start and end of the year, and the parameter p accounts for the slight linear decrease observed in the NDVI time series during the winter and summer seasons (Fig. 1).

For the deciduous species and based on the fitted NDVI time series, we derived 6 metrics for both spring (S_1 to S_3) and autumn (A_1 to A_3) seasons (Fig. 1). S_2 and A_2 are the dates of maximum increase and decrease of the NDVI (inflexion points) during the leaf expansion and leaf senescence phases, and they are directly given by u and v fitting parameters, respectively. The metrics S_1 and S_3 are the days of the year delimiting the leaf expansion phase in the spring. A_1 and A_3 are the days of year delimiting the leaf senescence phase in the autumn. $S_1, S_3, A_1,$ and A_3 are determined from the local extrema of the third derivative of the fitted NDVI time series (Soudani et al., 2008). Note that S_1, S_3 and A_1, A_3 correspond to the onset of the greenness increase, the onset of the greenness maximum, the onset of the greenness decrease and the onset of the greenness minimum, respectively, given in the MODIS Vegetation phenology product (MCD12Q2). S_2 and A_2 are not given in the MCD12Q2 product.

For evergreen species whose phenological characteristics exhibit little change through time, and for crops and savannahs whose phenological characteristics exhibit irregular temporal patterns that cannot be modeled by the ADS function (Eq. 2), we used cubic splines to

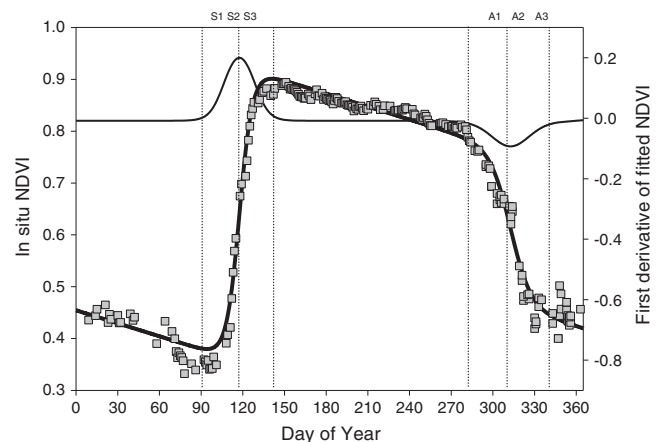


Fig. 1. In situ measured (gray square) and fitted NDVI time series (bold curve) over an oak forest stand in Fontainebleau during the year 2006. The rate of change given by the first derivative of the fitted NDVI time series (continuous curve – right axis). The vertical lines show six phenological markers derived from the fitted NDVI time-series (*S* and *A* refer to spring and autumn phenological events, respectively).

fit the NDVI time series because of their great flexibility for fitting data and because they are differentiable, allowing for the implementation of the following phenological date detection procedure:

- In a first step, the NDVI transition phases are localized by determining all local extrema. The duration of each phase is given by the duration between two successive extrema. Thus, each NDVI phase corresponds to a period of time where the NDVI varies in a monotonous manner.
- In a second step, all dates for which the ratio of the noise-to-signal metric described below (Section 2.5.1) is at a minimum and lower than the duration of the NDVI phase are considered as having a phenological significance. In other words, metrics that exhibit a noise-to-signal ratio higher than the duration of the NDVI transition phase were considered non-significant.

Fig. 2 illustrates an in situ NDVI time series over an evergreen forest.

For every site, the dates of phenological events detected using MODIS daily and MODIS 16-days were compared to those detected using in situ NDVI time-series.

2.5. Theoretical assessment of the predictive power of vegetation phenology from in situ and satellite-based NDVI time series

2.5.1. Predictive power of vegetation phenological markers derived from in situ and satellite-based NDVI time series

Uncertainties on the dates of phenological events derived from NDVI time series are determined as follows. The NDVI time series may be written as:

$$NDVI(t) = fNDVI(t) + \varepsilon \quad (3)$$

$fNDVI(t)$ is the signal given by the fitted curve (ADS or cubic spline), and ε (fitting error) is a random noise with zero mean. This last assumption is discussed below.

The total variance of NDVI around time t describes the total information (signal and noise) contained in $NDVI(t)$ and is given by the following equation (assuming independence between $NDVI$ and ε):

$$Var(NDVI) = Var(fNDVI(t)) + Var(\varepsilon) \quad (4)$$

$Var(fNDVI(t))$ may be locally approximated by:

$$Var(fNDVI(t)) \approx \left(\frac{dfNDVI(t)}{dt} \right)^2 * Var(\varepsilon) \quad (5)$$

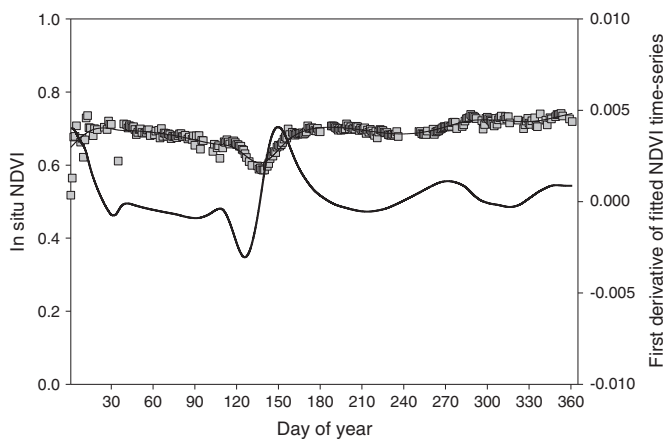


Fig. 2. In situ measured (gray square) and fitted NDVI time series using cubic splines (continuous curve) over an evergreen broadleaf forest in Puechabon during the year 2009. First derivative of the fitted NDVI time series (continuous curve – right axis).

$\left(\frac{dfNDVI(t)}{dt} \right)^2$ gives the NDVI variance per unit of time and may be used as a measure of the information in the NDVI signal observed at time t . $Var(\varepsilon)$ is the variance around time (t).

$Var(\varepsilon)$ corresponds to the variance of residuals between the predicted NDVI from the fit $fNDVI(t)$ and the observed NDVI values. $Var(\varepsilon)$ is equal to $RMSE(t)^2$ – i.e., the mean square error.

We define the predictive power of the NDVI time series locally at time (t) using the following expression:

$$pp(t) = \sqrt{\frac{RMSE^2}{\left(\frac{dfNDVI(t)}{dt} \right)^2}} \quad (6)$$

pp is expressed in days (time unit) and can be read as the number of days during which a monotonous variation in $NDVI(t)$ should continue until it exceeds the noise. Therefore, pp is the theoretical uncertainty estimation of a given date (t) based on the NDVI change from the NDVI fit and taking into account the noise in the data around the fit. More generally, it corresponds to the noise-to-signal ratio and expresses the number of days necessary to obtain an NDVI temporal change higher than the NDVI noise.

The denominator is the first derivative of the NDVI fit because the estimation of the phenological metrics is based on the detection of an NDVI increase or decrease. The numerator term ($RMSE$) measures the NDVI noise. The noise is assumed to be constant over the year. For deciduous forests, this assumption is not strong after modifying the ADS function according to Eq. (2). Indeed, the examination of the NDVI time series shows a slight monotonic decrease in the NDVI throughout the seasons of winter and summer. The two parameters p and e were introduced to homogenize the distribution of residuals around the fit. However, over evergreen forests, the distribution of the residuals around the fit is not always homogeneous, as the flexibility of the spline that is used is not sufficient to account for all of the NDVI signal variations, which are particularly fast and short.

Eq. (6) was used to assess the potential error around an estimated phenological metric over both deciduous and evergreen forests.

2.5.2. Sensitivity analysis of MODIS-derived phenological metrics to data gaps in NDVI time series

To estimate the influence of data gaps due to clouds and snow in remotely-sensed NDVI time series on the ability to predict phenological events, we artificially introduced data gaps with several different lengths in in situ NDVI time series.

In a first step, the probability density function (pdf) of clear sky in the year at the time of the MODIS overpass was established using measurements of the sunshine duration acquired using a BF3 sunshine sensor (Delta-T devices) at a half-hour time step in the Fontainebleau tower-flux site during the year 2008. The year 2008 may be considered as a “normal year” representative of the regional cloud cover regime. We defined a clear sky as that in which the sunshine duration is at least 10 min per 30 min of measurements using the BF3 sensor. The pdf of clear sky days was determined using a non-parametric kernel smoothing density estimation fitted to the empirical histogram of clear days (Fig. 3). The pdf determines the conditional probability that the sky will be clear at the time of the MODIS overpass on a given day of the year. For example, if it is assumed that half of the year is covered by clouds during the MODIS overpass and that all days are equally likely to be cloudy, then the probability of having a clear sky for a given day is: $(1/365) \times 0.5$.

In a second step, an in situ NDVI time series is used to randomly generate an NDVI time series with gaps. We generate an NDVI time series with between 30 and 189 observations according to the probability density function for clear sky determined above. For each length of the NDVI time series, this operation is repeated 100 times. As a result, a total of 16,000 NDVI time series were created. Then, the ADS

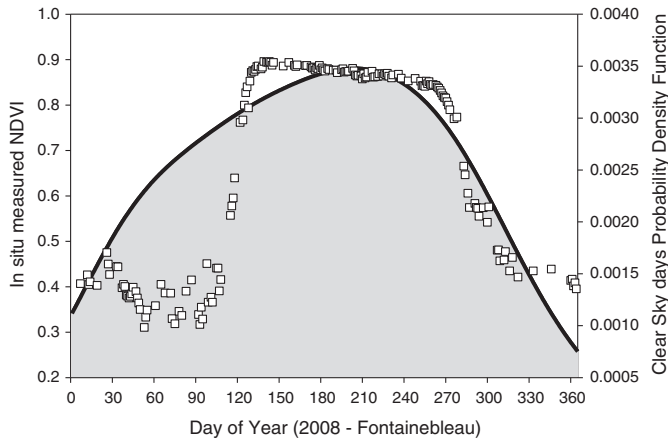


Fig. 3. In situ measured NDVI in Fontainebleau forest for the year 2008 (empty square, left axis). The filled area under the continuous curve is the probability density of clear sky for each day of the year (the sky is considered clear when the sunshine duration is at least 10 min per period of 30 min at the time of the MODIS overpass (right axis)).

(Eq. 2) was fitted to each sample of the simulated NDVI time series, and the six phenological metrics defined above were estimated.

To quantify the strength of the NDVI signal of each simulated NDVI time series, we calculate the first derivative of the fitted NDVI at the date of each NDVI observation of the dataset. The absolute values of the first derivatives averaged over the series are used as a simple measure of the NDVI signal strength. For example, for a time series composed of very close NDVI values, it is expected that the curve fitted to the NDVI time series will be flat, the first derivative calculated for each NDVI observation will be zero or close to zero and the average signal strength over all NDVI observations will also be zero or close to zero.

Finally, according to the strength of the NDVI signal, we grouped all samples into 100 classes using an unweighted pair group method with the arithmetic mean (Sokal & Michener, 1958). For each class, we determined the average length of the simulated NDVI time series within the class and the average RMSE between the estimates of the phenological marker determined from the simulated time series and full NDVI time series.

3. Results

3.1. Comparison between ground- and MODIS-based NDVI time series

Fig. 4 shows the overall comparison between the in situ, daily and 16-day MODIS NDVI data.

For all vegetation types, the MODIS NDVI values are generally higher than those measured by in situ sensors. For the deciduous forests, the overall agreement between in situ and MODIS NDVI data is very good ($R^2 = 0.91$, $p < 0.00$). In the holm oak forest at Puechabon, the relationship is highly scattered due to small temporal changes in the canopy foliage area compared to the magnitude of the noise affecting the NDVI signal, even after filtering ($R^2 = 0.13$, $p < 0.00$). In the tropical forest, no significant relationship could be found ($R^2 = 0$, $p > 0.75$). In the succession of crops in Lonzeé ($R^2 = 0.56$, $p < 0.00$) and in the savannah site ($R^2 = 0.45$, $p < 0.00$), the relationships between in situ and MODIS NDVI measurements are significant but noisy despite the high in situ NDVI temporal changes.

In the deciduous forests, the linear relationships between the in situ and daily MODIS NDVI and between the in situ NDVI and MODIS 16-day composite data are similar for all sites (Fig. 4). While both filtering methods – CVA-MVC and GMM – appear to perform equally well, the filtering method based on a GMM applied to the daily MODIS NDVI time series provides a better temporal resolution and, as expected, preserves the intermediate values, which generally correspond

to key phenological phases (leaf expansion and leaf senescence), as shown in Fig. 4.

While the filtered MODIS NDVI observations are linearly correlated to the in situ NDVI measurements for deciduous forests, the evergreen forests exhibit a high level of noise in regard to the low in situ NDVI variability. The noise levels as estimated using RMSE between the observed and fitted NDVI time series in the evergreen forest in the Puechabon and deciduous forests are similar (0.03 versus 0.04), and the lack of correlation is mainly due to a low NDVI temporal variability (low seasonal variation of phenology). In the tropical forest of French Guyana, no significant relationship could be found between the MODIS and in situ NDVI observations ($p > 0.75$). The RMSE is larger than in the deciduous forests (0.12 versus 0.04), possibly due to the effects of sub-pixel cloud contamination not detected by a MODIS cloud mask algorithm and a failure in the filtering process.

Despite the noise in the data, the in situ and MODIS data reproduce similar temporal patterns in deciduous forests (Fig. 5). The NDVI time series show with high temporal resolution the phenological seasonality of these species, which is characterized by two phases: the growing season from mid-spring to summer and the dormancy season during late autumn and winter. These main phases are separated by two short transition phases delimited by two main phenological events: the onset of greenness when budburst starts in the spring and the onset of senescence in the autumn.

For the evergreen broadleaf forest of Puechabon (Fig. 6), the in situ NDVI time series show clear phases of NDVI decrease during the spring despite small NDVI variations. This pattern is consistent with the phenology of the holm oak characterized by the partial foliage renewal each year from March to the middle of June. Note that in the Puechabon forest, an unexplained sensor dysfunction coinciding with strong rains explains the gap in NDVI measurements during the autumn of the year 2008. The MODIS daily and MODIS 16-day composite NDVI time series show small signal variations that do not coincide with the in situ NDVI measurements.

In the tropical forest (Fig. 7), in situ NDVI time series show two periods characterized by declines in the NDVI of variable magnitudes occurring around the middle of March for the first period and around days 300–320 (October) for the second period. For the first period, the decline in NDVI is clearly visible in 2007 and 2008. For the second period, the decline in NDVI appears only in 2008 and 2009. The first period of NDVI decline was much shorter than the second one. The second decline was more pronounced in 2009. Contrary to the in situ NDVI measurements, MODIS NDVI time series (Fig. 7) include so much noise that none of the tested filtering methods could provide a usable signal. The temporal pattern from the MODIS 16-day composite NDVI data is inconsistent with the in situ NDVI time series. This pattern is mainly characterized by two periods that coincide with the main rainy season from December to July (sometimes interrupted by a short dry season in March called the little summer of March) and the main dry season (July–November). The rainy season is characterized by abnormally low values of NDVI, and the second period is characterized by NDVI values at the same level as the daily MODIS NDVI data. This temporal pattern may arise from variations in noise intensity. As shown in Fig. 7, none of the tested filters could provide a good agreement between the in situ and MODIS observations.

During the succession of crops at the Lonzeé site (Fig. 8), the in situ NDVI measurements started in 2007 at the end of March, during the growth of winter wheat. For this crop, the in situ NDVI increases during the spring, reaches a peak at the end of April and then decreases during June and July to reach a minimum value a few weeks before the harvest at the beginning of August. After the harvest, the NDVI peaks again in the first week of September due to a re-growth of wheat and weeds. In 2008, during the growth of the sugar beet crop, the NDVI increases, reaches its maximum at the end of June and remains almost constant during the summer until the harvest at the beginning of November. In 2009, the in situ NDVI time series

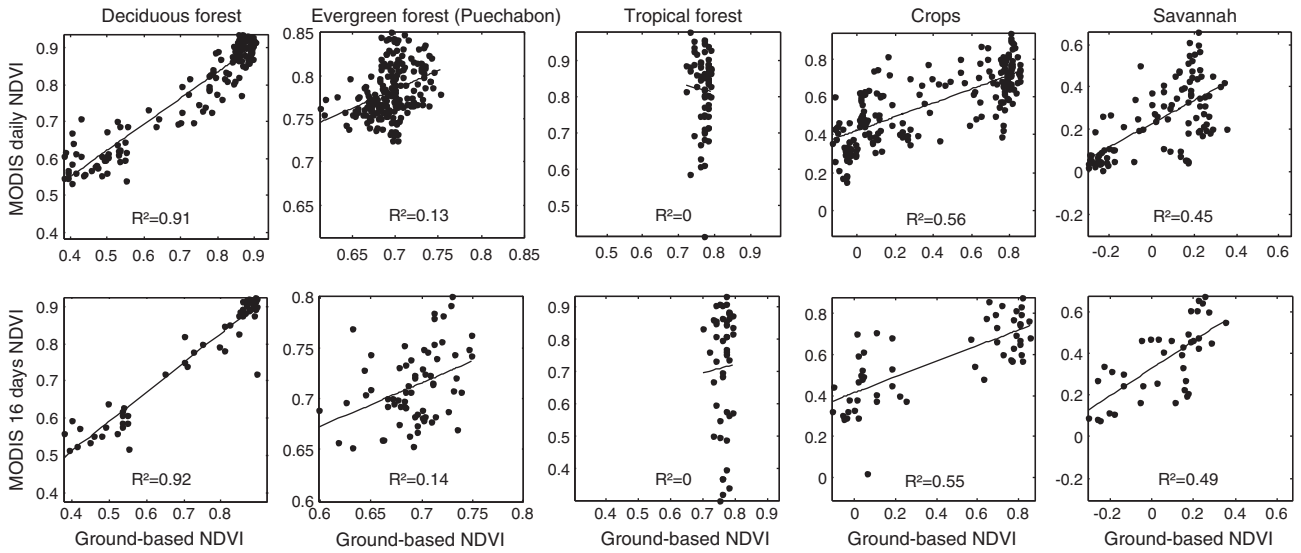


Fig. 4. In situ NDVI (x-axis) versus daily (upper figures) and 16-day composite MODIS NDVI data for the different biomes. R^2 : coefficient of determination.

is bimodal, reproducing the phenology of a succession of two crops of winter wheat and mustard.

In the succession of crops, the MODIS daily and 16-day composite signals (Fig. 8) exhibit strong noise, but the main temporal patterns associated with the phenology of this vegetation could be identified.

In the grass savannah at the Tchizalamou site (Fig. 8), the temporal patterns of the in situ NDVI measurements in 2008 and 2009 are similar, with the exception that the NDVI remains high during February and March 2009. The NDVI is at its maximum during the main wet season from October to May and at its minimum during the main dry

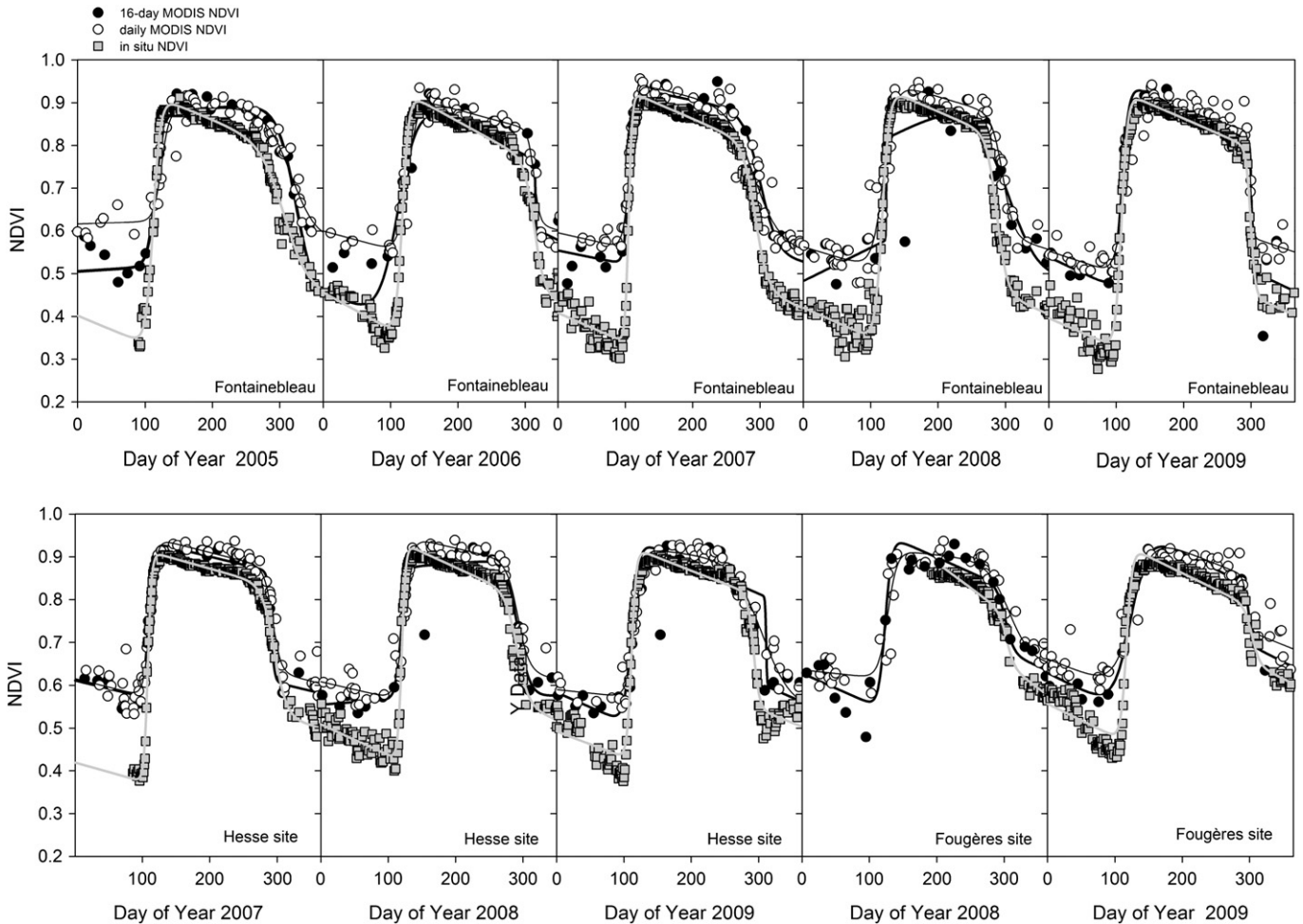


Fig. 5. Time series of in situ NDVI (gray squares), daily MODIS NDVI (empty circles) and 16-day composite MODIS NDVI (filled circles) over deciduous forests.

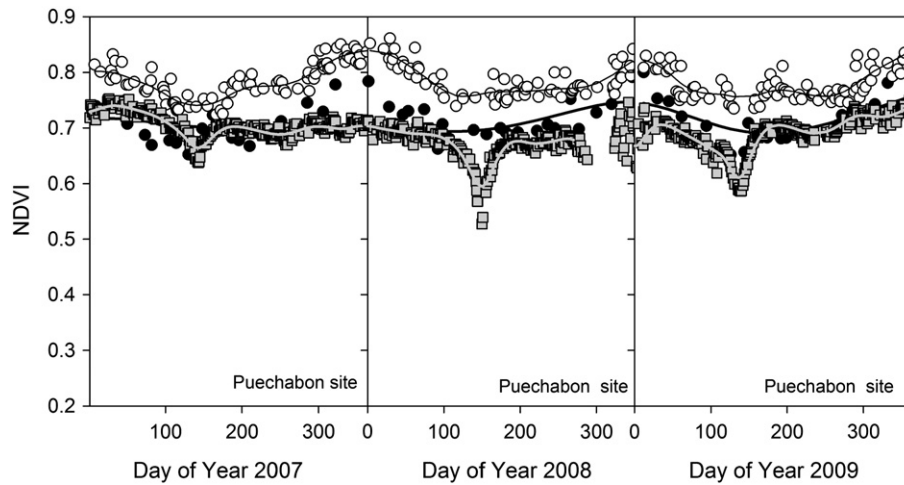


Fig. 6. Time series of in situ NDVI (gray squares), daily MODIS NDVI (empty circles) and 16-day composite MODIS NDVI (filled circles) over an evergreen broadleaf forest in Puechabon. The continuous curves represent the series of cubic splines fitted to the NDVI data.

season from May to October. The first decrease of the NDVI in 2008 is due to a short dry season, which may occur in February–March. For the two years, the sudden drop of NDVI at the end of the wet season is due to human-induced fire. Nevertheless, it is important to note that the mismatch between the in situ and MODIS observations in the savannah site occur during both rainy and dry seasons, and it is most likely due to contamination of the data by clouds that are not detected by the filtering process.

3.2. Comparison of phenological metrics estimates derived from in situ and MODIS daily NDVI time series

For the deciduous species, the comparative analysis for the 6 considered phenological metrics are shown in Fig. 9 and Table 2.

The best agreement between the predictions of the phenological dates based on the MODIS time series and in situ NDVI measurements is found for the two inflexion points S_2 and A_2 during the leaf expansion and the leaf senescence phases, respectively. The bias between the MODIS predictions and those based on in situ NDVI measurements is positive for S_2 , S_3 , A_2 , and A_3 (MODIS-based phenological markers occur later). It is less important for S_2 and A_2 than for S_3 and A_3 , which delimit the end of the two phases, i.e., the end of the leaf expansion

phase in the spring (S_3) and the end of the leaf senescence phase in the autumn (A_3). In comparison with the daily MODIS series, the bias for S_2 is positive at approximately 4 days, and it is also positive for A_2 at 2.5 days. On both sides of the two inflexion points, the bias is negative for S_1 in early spring (MODIS-based phenology estimates are earlier) and positive for S_3 at the end of the leaf expansion phase. Furthermore, it is negative for A_1 in early autumn and positive for A_3 at the end of the leaf senescence phase. The relationships between the ground-based and MODIS daily spring metrics (S_1 , S_2 , S_3) are statistically significant ($p < 0.01$), while no statistically significant relationship could be found for the autumn metrics (A_1 , A_2 , A_3). The metrics derived from the MODIS 16-day series exhibit lower R^2 , and only the S_2 and S_3 metrics could be significantly related to the ground-based metrics ($p < 0.02$ and $p < 0.04$, respectively).

3.3. Theoretical analysis of the predictive power of NDVI time series for phenology detection

Because the phenological metrics are based on the derivatives of the fitted NDVI time series, the RMSE of the first derivative ratio was used to quantify the expected theoretical uncertainty of any particular phenological metric regardless of the signal noise (Eq. 6). As described above, we

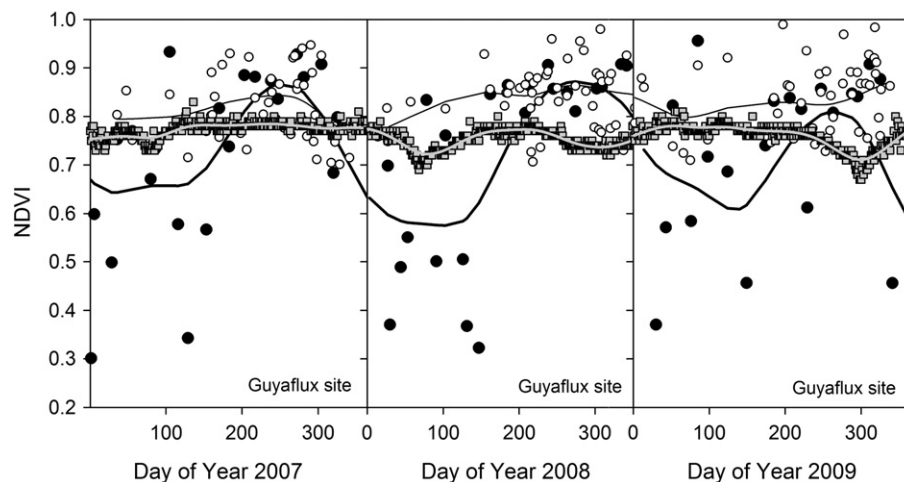


Fig. 7. Time series of in situ NDVI (gray squares), daily MODIS NDVI (empty circles) and 16-day composite MODIS NDVI (filled circles) over the tropical forest in French Guyana. Continuous curves represent the series of cubic splines fitted to the NDVI data.

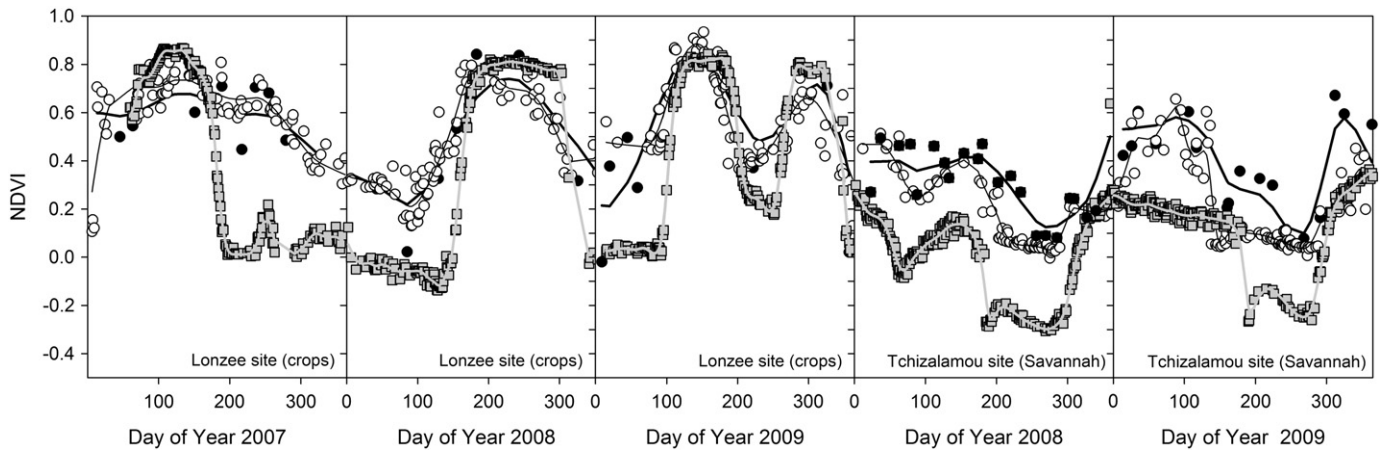


Fig. 8. Time series of in situ NDVI (gray squares), daily MODIS NDVI (empty circles) and 16-day composite MODIS NDVI (filled circles) over herbaceous species in Lonzeé (succession of crops) and at the Tchizalamou site (African savannah). Continuous curves represent the series of cubic splines fitted to the NDVI data.

recall that this ratio corresponds to the number of days needed to obtain an NDVI temporal change higher than the NDVI noise. Fig. 10A and B illustrates the application of this method to track features and to estimate the uncertainties (in days) of main phenological metrics in a deciduous forest in Fontainebleau and in an evergreen forest in Puechabon (Fig. 10).

Summary statistics of uncertainty in the main phenological metrics over all deciduous forests and for all years are provided in Table 3.

The uncertainties of phenological dates determined from the MODIS daily and 16-day NDVI products are similar. Nevertheless, the standard deviation is larger using the MODIS 16-day NDVI time series. In comparison with the in situ NDVI-derived phenological metrics, the theoretical uncertainty based on the daily and MODIS 16-day composite NDVI observations is higher, particularly for phenological markers associated with autumn. The phenological dates given by the inflexion points during the leaf expansion phase in the spring and the leaf senescence phase in the autumn are significantly more accurate than the other metrics. This result is of great importance because it demonstrates that the inflexion point metric is more robust for tracking the phenology from the NDVI time series in temperate broadleaf deciduous forests.

For the other biomes, summary statistics of uncertainty assessed over evergreen forests, savannah and crops are provided in Table 4.

For crops and the herbaceous savannah, the uncertainties obtained for the most significant transition dates derived from the in situ NDVI time series are comparable to those obtained for deciduous forests. For the evergreen forest of holm oak and the rainforest, the uncertainties are higher, differing from in situ NDVI measurements by approximately

10 days. In contrast, the daily and 16-day MODIS NDVI time series are not able to describe the phenology of these ecosystems with sufficient accuracy.

3.4. Influence of data gaps in the MODIS NDVI time series on the prediction accuracy of phenological metrics in deciduous forests

Based on the Fontainebleau 2008 in situ NDVI time series considered as a reference and by inserting artificial gaps into the actual data using the method described in Section 2.5.2, Fig. 11 shows the differences between the phenological estimates from the full NDVI time series and the simulated (with data gaps) NDVI time series for the different phenological markers defined in Fig. 1.

In Fig. 11, the abscissa (x-axis) corresponds to the mean of the absolute values of the first derivatives of ADS fitted to the simulated NDVI time series. The first derivative is numerically calculated for every day of NDVI observation. Low values of the x-axis represent a loss of information (loss of NDVI signal) due to a bad compositing of the NDVI time series (decrease of the proportion of informative observations that are acquired during leaf expansion and leaf senescence phases), while the increase represents a relative gain of information due to the removal of uninformative observations (i.e., NDVI values during the winter and summer seasons). The two ordinate axes (left y-axis and right y-axis) correspond to the average RMSE between the estimates of the phenological marker determined from the simulated and full NDVI time series (left y-axis) and the average length of the simulated NDVI time series (right y-axis).

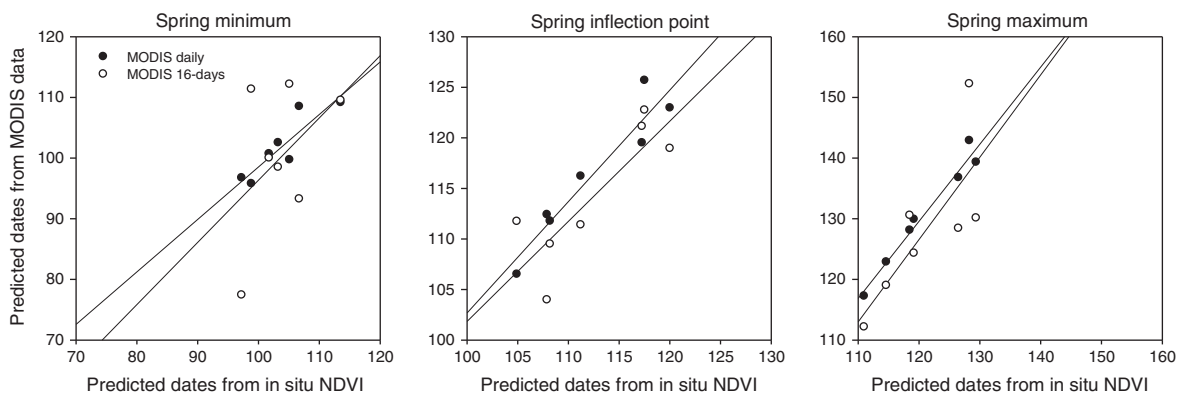


Fig. 9. In situ NDVI-derived metrics (day of year) versus MODIS NDVI-derived metrics (day of year) for deciduous forests.

Table 2
Comparison between the phenological metrics derived from the in situ NDVI measurements (considered as reference) and MODIS data. (S_1, S_2, S_3) for the spring and (A_1, A_2, A_3) for the autumn. MAE (days): mean absolute error, bias (days): (+) MODIS overestimation, (–) underestimation, RMSE (days): root mean square error. R^2 : coefficient of determination of the regression between the phenological markers based on the in situ and MODIS NDVI time series. Significant values are noted in bold ($p < 0.05$).

	S1		S2		S3		A1		A2		A3	
	MODIS daily	MODIS 16-day	MODIS daily	MODIS 16-day	MODIS daily	MODIS 16-day	MODIS daily	MODIS 16-day	MODIS daily	MODIS 16-day	MODIS daily	MODIS 16-day
MAE	2.5	9	4	3	10	7	11	11	4	5.5	15	12
Bias	–2	–3.5	4	1.5	10	7	–4	7.5	2.5	4	9	0.5
RMSE	3.	11	4.5	4	10	10.5	14.5	14	6	8	22	14
R^2	0.8	0.2	0.9	0.7	0.97	0.59	0.42	0.76	0.56	0.47	0.04	0.01
p	0.007	0.312	0.001	0.019	0.000	0.043	0.115	0.102	0.052	0.09	0.668	0.825

The general form of the relationships between the RMSE and the mean of the absolute values of the first derivatives of the fitted NDVI time series is concave up. The RMSE is minimal around the middle of the x-axis and then increases rapidly on both sides for low and high values. In contrast, the general form of the relationships between the average length of simulated NDVI time series and the x-axis is concave down, indicating that the prediction errors of phenological metrics are lowest when the length of the simulated NDVI time series is high.

In Fig. 11, both the level and the extent of the central part of the RMSE curve, characterized by stable and low values, vary according to the phenological metric considered. The RMSE is lower and the region of error stability is wider for phenological metrics based on the inflexion points (S_2 and A_2) during the spring and autumn, respectively. For the spring phenological metrics, the point of inflexion S_2 is subject to the smallest error (<1 day) for a length of NDVI time series varying between 35 and 140 observations. For the autumn phenological metrics, the prediction error at the point of inflexion (A_2) is higher and less stable at approximately 3 days for a range of sample sizes varying from 60 to 140 observations.

The extent of the portion of the curve where the RMSE is stable indicates the sensitivity of the phenological metrics to the length of the NDVI time series and to signal degradation due to cloud cover. Table 5 gives the range of the length of the simulated NDVI time series that bounds the region of RMSE stability (defined as the region having the lowest RMSE ± 1 day). This range gives the minimum number of NDVI observations retained without significantly degrading the predictive quality of the NDVI time series.

The results in Table 5 show that the average length of the simulated NDVI time series is considerably lower for S_2 and A_2 than for the other metrics, indicating that the phenological metrics based on the inflexion points are less sensitive to data gaps and signal degradation due to cloud cover. The prediction error remains at its minimum by keeping only approximately 27% and 40% of the total number of NDVI observations in the best case (gaps or cloudy observations concentrated

during the summer and winter) or approximately 40% and 61% of the total number of observations in the worst case (gaps or cloudy observations concentrated during the spring or autumn).

4. Discussion

In situ NDVI measurements are made only a few meters above the canopy, and because NDVI is a normalized index, the effects of the sky conditions produce little noise. In situ NDVI measurements can thus be carried out under diffuse sky conditions, allowing for the monitoring of vegetation phenology at high temporal frequency in deciduous and evergreen forests for which the phenological variations are less pronounced. These data may be considered as a reference offering adequate empirical and theoretical frameworks for directly assessing the potential use of satellite data to predict vegetation phenology in different biomes and under different sky conditions. Nevertheless, when comparing coarse satellite data to ground measurements, spatial heterogeneity can become an important source of uncertainty in predicting phenology if certain precautions are not taken. In this study, the ground-based NDVI measurements benefited from an existing network of seven eddy covariance flux towers that were installed on flat terrain with relatively homogeneous vegetation cover, specifically chosen to satisfy the assumptions of the eddy covariance method and to avoid scaling issues and plant species heterogeneity (Chen et al., 2009; Metzger et al., 2012). In addition, for each study site, the homogeneity of the vegetation composition within the MODIS 250 m pixel was checked by visual photo-interpretation complemented by the use of Landsat TM/ETM+ based NDVI subsets and ancillary ground-based observations. Nevertheless, it is important to note that these precautions do not completely remove the residual uncertainty due to the spatial heterogeneity in the MODIS pixel. We emphasize that ground-based NDVI measurements are acquired at a constant viewing angle, while MODIS data are acquired with different viewing geometries. BRDF effects lead to uncertainties of variable magnitude in the seasonal course of surface reflectance,

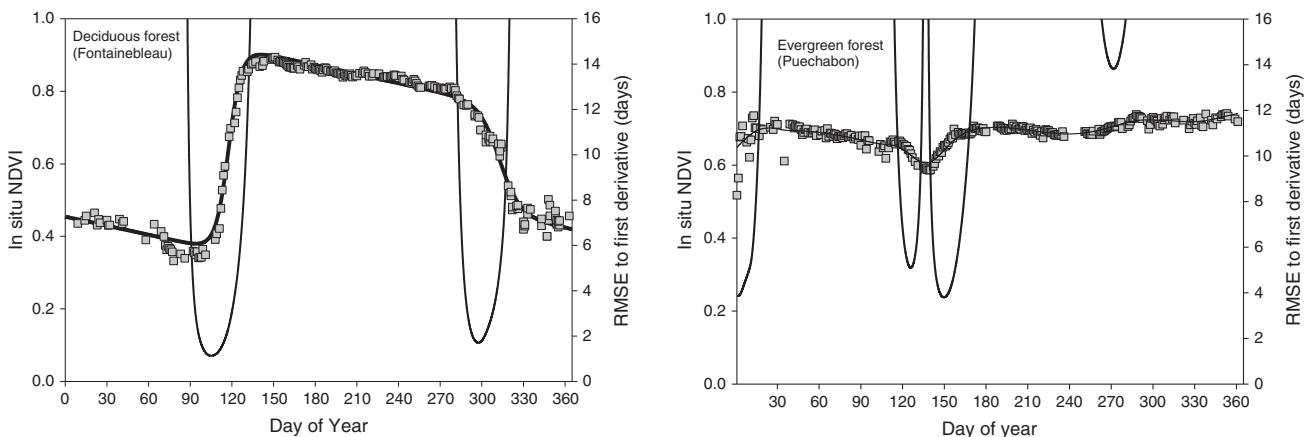


Fig. 10. In situ measured (gray squares) and fitted NDVI time series over a deciduous forest in Fontainebleau for year 2006 (left) and over an evergreen broadleaf forest of holm oak in Puechabon forest (right) during the year 2009. The continuous curve is the ratio between the RMSE and first derivative (right axis).

Table 3

Average and standard deviation of the theoretical uncertainties (from Eq. 6) calculated for six phenological metrics (Fig. 1) derived from the fitted NDVI time series over deciduous species and for all years (sample size = 10). (S_1, S_2, S_3) for the spring and (A_1, A_2, A_3) for the autumn.

	Theoretical uncertainty (days)	S1	S2	S3	A1	A2	A3
In situ NDVI	Average	2	0.7	2	6.5	2.5	6.0
	Standard deviation	2.5	0.7	2.5	6.5	2.5	6.5
MODIS daily NDVI	Average	7.5	2	7.5	13	5	13
	Standard deviation	8.5	2.5	8.5	16.5	6	16.5
MODIS 16-day NDVI	Average	8	2.5	8	14	5	14
	Standard deviation	12	3.5	12	22	7	22

and they may cause bias in the identification of vegetation phenological events (Fensholt et al., 2010; Hird & McDermid, 2009; Sims et al., 2011; Tan et al., 2006). In this study, we used the MODIS 16-day product derived from the CVA-MVC compositing methodology that preferentially select highest NDVI values with zenith view angle closest to nadir view (Huete et al., 2002). No specific constraint on the viewing angle has been applied to daily MODIS data previously. Nevertheless, daily 250 m MODIS NDVI data were previously filtered using GMM and a moving-window mean filter to minimize the total noise due to variations in the atmospheric conditions, mismatch in the spatial scales between the MODIS data sets, and differences in radiometric data acquisition geometry.

In this study, a new filtering method based on mixture Gaussian models has been developed to remove spurious MODIS NDVI data in deciduous forests without altering their phenological patterns. This method showed good performance in terms of the similarity between the in situ and daily MODIS NDVI time series (Fig. 5). However, in evergreen forests, this method has a limited efficiency for filtering daily and 16-day MODIS NDVI time series because the magnitude of noise is of the same order as the phenological signal (Figs. 6 & 7).

After the removal of spurious NDVI observations, both MODIS and in situ NDVI time series allow us to predict with good accuracy the two main phenological events in temperate deciduous forests: the date of the onset of greenness in the spring and the date of the onset of leaf senescence in the autumn (Fig. 9, Table 2). The MODIS daily NDVI derived onset of greenness metrics was shown to be well correlated to the in situ NDVI metrics, while the related senescence metrics may still be challenging. The use of the MODIS 16-day NDVI series yielded more variable results, which is probably due to the loss of intermediate NDVI values.

The inflexion points during NDVI increase and NDVI decrease phases in the spring and autumn constitute the best predictors in terms of robustness to data gaps and prediction accuracy. These results are in agreement with Fisher et al. (2006), Soudani et al. (2008), and Busetto et al. (2010). For inflexion-point-based phenological metrics, the biases between in situ and MODIS-based NDVI time series estimates are positive and vary between 2 and 4 days for the daily and 16-day composite MODIS NDVI time-series, respectively. For the spring minimum (S_1) and autumn maximum (A_1) metrics derived from the daily MODIS time series (Table 2), the biases are negative, meaning that MODIS tends to detect the onset of greenness earlier. Negative bias in S_1 was also reported by Fisher et al. (2006) and Soudani et al. (2008). This result can be explained by the greater sensitivity of (S_1, S_3) and (A_1, A_3) to a lack of NDVI observations during short periods at the beginning

Table 4

Average theoretical uncertainty (from Eq. 6) for the significant phenological transitions derived from the fitted NDVI time series over crops, herbaceous savannah and evergreen forests.

	Theoretical uncertainty (days)	Savannah	Crops	Evergreen forests
In situ NDVI	Average	3.5	2.5	9.1
MODIS daily NDVI	Average	6.6	10.5	19.5
MODIS 16-days NDVI	Average	13.5	24.2	162.5

and end of the leaf expansion and leaf yellowing phases, respectively. A lack of NDVI measurements has the effect of shifting the start of the sigmoid to the left at S_1 and A_1 and to the right at S_3 and A_3 . This point will be discussed in detail below.

The use of the method based on the noise-to-signal ratio developed in this study (Eq. 6) provided a quantitative insight about the uncertainty of each phenological metric and its reliability, accounting for the initial NDVI signal, filtering, and fitting techniques in both deciduous and evergreen forests. In deciduous forests (Table 3), whether the data were obtained from the in situ or MODIS NDVI time series, the theoretical uncertainty yielded significantly lower values for the phenological transition dates based on the inflexion points for both spring and autumn phases. This result may be explained by two reasons. First, the rate of change of the NDVI during these two periods is higher, and thus, the noise-to-signal ratio is lower, allowing a better fit of the data. Second, the inflexion point of the NDVI curve is more stable due to the constraint of symmetry around this position. During the leaf expansion phase, this date is constrained by two NDVI plateaus in the winter and summer. During leaf senescence, it is constrained by two other plateaus in the summer and autumn/winter. For these two reasons, a relatively small number of NDVI measurements that are of good quality and are well distributed over the seasons (winter, leaf expansion and senescence phases, summer and autumn) may be sufficient to obtain good estimates. The dates of the NDVI minimum increase and the NDVI maximum are not constrained, and it is necessary to have high-quality NDVI data during these periods to obtain accurate estimates.

The conclusions underlined above are confirmed by the results of the sensitivity analysis of the phenological markers to the lack of NDVI data conducted on the 2008 year in Fontainebleau site, which exhibit strong phenological pattern and low noise, as summarized in Fig. 11 and Table 5. The dates of spring and autumnal phenological transitions derived from inflexion points are the most accurate and most robust. The use of the inflexion point may even be necessary to estimate the date of leaf senescence with sufficient accuracy because of the strong instability of the other two indices (A_1 and A_2), as shown in Fig. 11 and Table 5. However, during the autumnal phase, the NDVI decline is generally slower and less pronounced than during leaf expansion in the spring because it depends on biological and physical mechanisms (leaf yellowing, browning, leaf fall, marcescence, and the mechanical influence of wind and precipitation) that may vary from year to year. Marcescence, which means that leaves die but do not fall off of trees in the autumn, is frequent in temperate deciduous forests and may influence the NDVI decline. In addition, it is highly likely that the contribution of the soil covered with newly fallen leaves may also significantly affect the NDVI signal and may explain (at least partially) the slow decline of the NDVI during the autumn and throughout the winter, as shown in previous studies (Nagler et al., 2000; Van Leeuwen & Huete, 1996). These factors may shift the position of the inflexion point to the right and cause an overestimation of the date of leaf yellowing and senescence in the autumn.

The results of the sensitivity analysis (Fig. 11) also show that the inflexion point is the most robust remote sensing-based phenological metric to gaps in the NDVI time series. The spring phenological transition prediction error remains less than one week when the number of

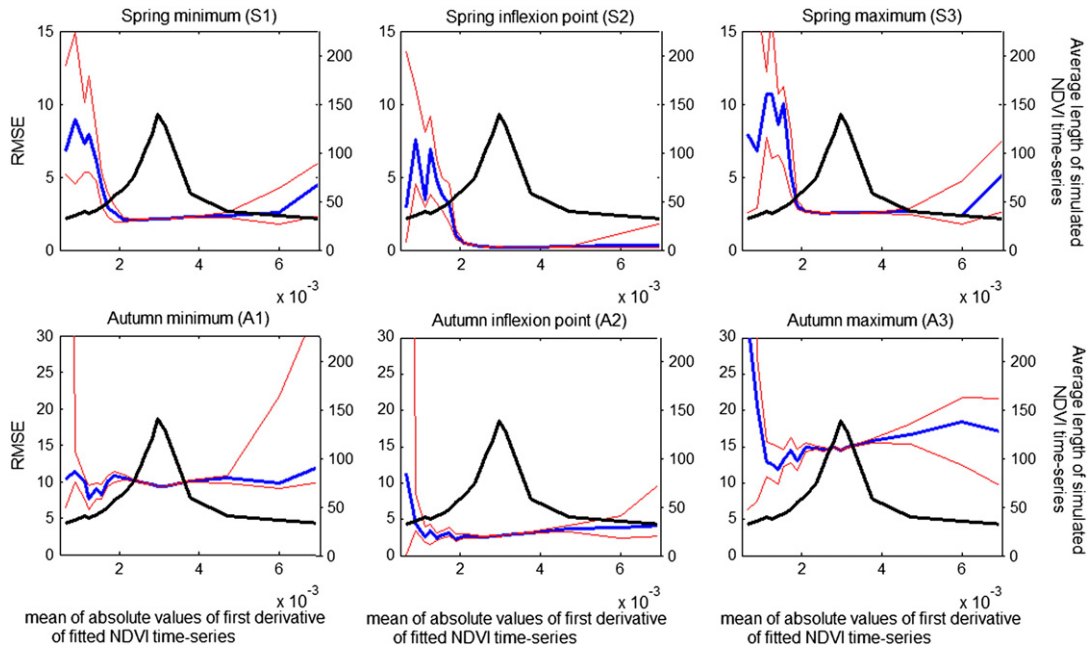


Fig. 11. Relationships of phenology prediction error (days) (blue line, left y-axis) and the length of the simulated NDVI time-series (black line – right y-axis) versus the average of the absolute values of the first derivatives of fits of simulated NDVI time-series (x-axis). The red lines are the confidence limits (95%) of the phenology prediction error.

NDVI observations is less than 30, corresponding to one observation every two weeks, which is equivalent to the multi-temporal MODIS NDVI 16-day composite product. This leads us to the conclusion that the MODIS 16-day composite NDVI data may allow accurate predictions of spring phenology using the inflexion point of the NDVI curve provided that the NDVI observations are not contaminated by clouds and that they are well distributed over the main transition phases. When those two conditions are not met, the use of MODIS 16-day composite NDVI may lead to hazardous prediction, as shown in the left part of the graphs (Fig. 11). However, it is difficult to predict the timing of autumn phenological transition with one week of accuracy using the MODIS 16-day NDVI data, and it is still highly unlikely that such accuracy can be achieved by using the criteria A_1 and A_3 , even when the MODIS daily NDVI data are used (Table 3).

In the evergreen forest in Puechabon and the tropical rainforest (Figs. 6, 7 & Table 4), the in situ NDVI time series show low NDVI variations. In the evergreen Mediterranean forest of holm oak, the NDVI variations are consistent with the phenology of this species, which is mainly characterized by two major events: the sprouting of leaves and shoots in the spring and the shedding of leaves, which is particularly important during the phase of leaf sprouting in the spring and occasionally autumn (La Mantia et al., 2003; Soudani et al., 2012). In the tropical rainforest in French Guiana, the interpretation of the NDVI temporal patterns is more complex because of the high species diversity in such forests. Nevertheless, the two periods of NDVI decline, which are observed occasionally during the first short dry season in February–March and during the second (main) dry season from the end of August to the end of October, are concomitant with two periods of lower rainfall

and higher solar radiation. The NDVI decline during the second dry season coincided with a peak of litterfall, as shown by measurements of the litterfall regime based on the use of litter traps placed beneath the canopy in this forest (Soudani et al., 2012).

The seasonal phenological features derived from the daily MODIS NDVI time series measured over the evergreen forests are quite poor because only a slight decrease of the NDVI in the spring in the Puechabon forest was detected. However, 16-day composite MODIS NDVI time series could not provide a sufficient certainty to precisely detect any of the phenological features of the evergreen forests.

In the tropical forest (Fig. 7), the MODIS NDVI time series exhibited strong noise, so none of the temporal features detected in ground-based NDVI time series could be found in the MODIS NDVI data. In contrast, the wave shapes observed in the 16-day composite and daily (with a lower magnitude for the latter) NDVI time series are mainly driven by seasonal variations in noise intensity. We note that during the main dry season, this pattern is opposite to that observed in the in situ NDVI time series. It is also important to note that the seasonal patterns of the MODIS 16-day composite NDVI shown in Fig. 7 are similar to those obtained in previous works (Huete et al., 2006; Saleska et al., 2007). These studies concluded that there is an increase in the canopy greenness during dry periods. Our results suggest that this pattern may not reflect a phenological signal but a variation of the noise intensity in the NDVI observations. The use of the MODIS daily or 16-day composite data without any ground-based reference may therefore be misleading.

The results from the savannah and crop sites (Fig. 8, Table 4) pinpoint an important limitation of the MODIS NDVI time series in the detection phenological features: while the actual features were detected, strong

Table 5
Sample sizes defining the stability region of the root mean square errors (lower RMSE \pm 1 day) of the phenological estimates in deciduous forests due to the introduction of artificial data gaps in the NDVI time series (first line). (Second line): Proportions of the remaining NDVI data (percentage of the total number of observations of the entire in situ NDVI time series, $n = 189$). (S_1, S_2, S_3) for the spring and (A_1, A_2, A_3) for the autumn. * [left–right] corresponds to both sides of the stability region for each phenological metric (see Fig. 11).

Phenological metrics:	S1	S2	S3	A1	A2	A3
Average length of simulated NDVI time series (n) [left–right*]	83–73	75–51	94–97	124–118	115–73	139–98
(In % of full NDVI dataset) [left–right]	44%–39%	40%–27%	49%–51%	65%–62%	61%–40%	73%–51%

errors occurred due to mixed pixels or bad sky conditions coinciding with phenological events. These errors could not be addressed by the tested filters or by the noise-to-signal ratio. At the savannah site, which may be heterogeneous at the MODIS pixel scale, some comparable features could be found between the in situ and MODIS series such as the NDVI drop due to a short dry period in March 2008, and the green-up at the end of 2009, while there were localized mismatches, notably around June, when the area is burnt. This observation may indicate a possible scale mismatch between the in situ and MODIS observations.

5. Conclusion

In this study, in situ NDVI time series allowed us to directly assess the accuracy of MODIS-derived phenological estimates. In deciduous forests, inflexion points of a double sigmoid model fitted to NDVI data allow for the most accurate estimates of the onset of greenness in the spring and the onset of yellowing in the autumn (RMSE \leq one week). Phenological metrics delimiting the leaf expansion phase in the spring and the leaf senescence phase in the autumn, which are identical to those provided in MODIS Global Vegetation Phenology product (MDC12Q2), are less robust to data gaps, and they can be subject to large biases of approximately two weeks or more during the autumn phenological transitions. The inflexion point detection was shown to be more precise and less sensitive to data gaps than these metrics. However, the use of the date at the beginning of the NDVI decline in the autumn (identical to the onset of the greenness decrease in MDC12Q2) instead of the date at the inflexion point can be justified because of the slow, monotonic decline of the NDVI during the autumn and winter, which could be due to the contribution of freshly fallen leaf litter and because the phenomenon of marcescence can cause a shift to the right of the inflexion point that could lead to overestimation of the onset of leaf yellowing. In the evergreen forests, in situ NDVI time series describe the phenology with high fidelity despite small temporal changes in the canopy foliage. However, MODIS is unable to provide consistent phenological patterns. In savannah and crops, the detection of phenological patterns could be achieved but was hampered by a seasonal variation of noise amplitudes. Similarly, in the tropical rainforest, the temporal pattern exhibited in the MODIS 16-day composite NDVI time series is more likely due to a pattern of noise in the NDVI data, structured according to both rainy and dry seasons rather than to phenological changes. More investigations are needed, but in all cases, this result leads us to conclude that the MODIS time series in tropical rainforests should be interpreted with great caution.

Acknowledgments

The authors thank GIP ECOFOR and F-ORE-T «Observatoires de Recherche en Environnement (ORE) sur le Fonctionnement des Écosystèmes Forestiers» ECOFOR, INSU, Ministère de l'Enseignement Supérieur et de la Recherche for funding the project that enabled manufacturing and deployment of the NDVI sensors in different vegetation types. The last author would also like to thank the University of Paris Sud for the PhD grant given to Mr Gabriel Hmimina. We would like to express our profound gratitude to Laurent Vanbostal and Daniel Berveiller for their help in manufacturing the NDVI sensors and measurements. We also thank all those involved in the data collection process at all study sites. We are very grateful for the thorough and helpful comments from the reviewers of the manuscript.

Appendix A. Supplementary data

Supplementary data associated with this article can be found in the online version, at <http://dx.doi.org/10.1016/j.rse.2013.01.010>. These data include Google map of the most important areas described in this article.

References

- Aubinet, M., Moureaux, C., Bodson, B., Dufranne, D., Heinesch, B., Suleau, M., et al. (2009). Carbon sequestration by a crop over a 4-year sugar beet/winter wheat/seed potato/winter wheat rotation cycle. *Agricultural and Forest Meteorology*, 149, 407–418.
- Beck, P. S. A., Atzberger, C., Høgda, K. A., Johansen, B., & Skidmore, A. K. (2006). Improved monitoring of vegetation dynamics at very high latitudes: A new method using MODIS NDVI. *Remote Sensing of Environment*, 100, 321–334.
- Bonal, D., Bosc, A., Goret, J. Y., Burban, B., Gross, P., Bonnefond, J. M., et al. (2008). The impact of severe dry season on net ecosystem exchange in the Neotropical rainforest of French Guiana. *Global Change Biology*, 14, 1917–1933.
- Box, J. E., Bromwich, D. H., Veenhuis, B. A., Bai, L. S., Stroeve, J. C., Rogers, J. C., et al. (2006). Green land Ice Sheet Surface Mass Balance Variability (1988–2004) from calibrated Polar MM5 Output. *Journal of Climate*, 19, 2783–2800.
- Busetto, L., Colombo, R., Migliavacca, M., Cremonese, E., Meroni, M., Galvagno, M., et al. (2010). Remote sensing of larch phenological cycle and analysis of relationships with climate in the Alpine region. *Global Change Biology*, 16, 2504–2517.
- Castaldi, S., de Grandcourt, A., Rasile, A., Skiba, A., & Valentini, R. (2010). Fluxes of CO₂, CH₄ and N₂O from soil of burned grassland savannah of central Africa. *Biogeosciences Discussions*, 7, 4089–4126.
- Chen, B., Black, T. A., Coops, N. C., Hilker, T., Trofymow, (Tony) J. A., & Morgenstern, K. (2009). Assessing tower flux footprint climatology and scaling between remotely sensed and Eddy covariance measurements. *Boundary-Layer Meteorology*, 130, 137–167.
- Chen, J., Jönsson, P., Tamura, M., Gu, Z., Matsushita, B., & Eklundh, L. (2004). A simple method for reconstructing a high-quality NDVI time series data set based on the Savitzky–Golay filter. *Remote Sensing of Environment*, 91, 332–344.
- Delbart, N., Le Toan, T., Kergoat, L., & Fedotova, V. (2006). Remote sensing of spring phenology in boreal regions: A free of snow-effect method using NOAA-AVHRR and SPOT-VGT data (1982–2004). *Remote Sensing of Environment*, 101, 52–62.
- Delpierre, N., Soudani, K., François, F., Köstner, B., Pontailler, J. Y., Aubinet, M., et al. (2009). Exceptional carbon uptake in European forests during the warm spring of 2007: A data-model analysis. *Global Change Biology*, 15, 1455–1474.
- Dufranne, D., Moureaux, C., Vancutsem, F., Bodson, B., & Aubinet, M. (2011). Comparison of carbon fluxes, growth and productivity of a winter wheat crop in three contrasting growing seasons. *Agriculture, Ecosystems & Environment*, 141, 133–142.
- Fensholt, R., Sandholt, I., Proud, S. R., Stisen, S., & Rasmussen, M. O. (2010). Assessment of MODIS sun-sensor geometry variations effect on observed NDVI using MSG SEVIRI geostationary data. *International Journal of Remote Sensing*, 31, 6163–6187.
- Fisher, J. I., Mustard, J. F., & Vadeboncoeur, M. A. (2006). Green leaf phenology at Landsat resolution: Scaling from the field to the satellite. *Remote Sensing of Environment*, 100, 265–279.
- Ganguly, S., Friedl, M. A., Tan, B., Zhang, X., & Verma, M. (2010). Land surface phenology from MODIS: Characterization of the Collection 5 global land cover dynamics product. *Remote Sensing of Environment*, 114, 1805–1816.
- Goerner, A., Reichstein, M., & Rambal, S. (2009). Tracking seasonal drought effects on ecosystem light use efficiency with satellite-based PRI in a Mediterranean forest. *Remote Sensing of Environment*, 113, 1101–1111.
- Granier, A., Bréda, N., Longdoz, B., Gross, P., & Nao, J. (2008). Ten years of fluxes and stand growth in a young beech forest at Hesse, North-eastern France. *Annals of Forest Science*, 65(7), 704.
- Heidinger, A. K., Anne, V. R., & Dean, C. (2001). Using MODIS to estimate cloud contamination of the AVHRR data record. *Journal of Atmospheric and Oceanic Technology*, 19, 586–601.
- Hird, J., & McDermid, G. J. (2009). Noise reduction of NDVI time-series: An empirical comparison of selected techniques. *Remote Sensing of Environment*, 113, 248–258.
- Huete, A. R., Didan, K., Miura, T., Rodriguez, E. P., Gao, X., & Ferreira, L. G. (2002). Overview of the radiometric and biophysical performance of the MODIS vegetation indices. *Remote Sensing of Environment*, 83, 95–213.
- Huete, A. R., Didan, K., Shimabukuro, Y. E., Ratana, P., Saleska, S. R., Hutrya, L. R., et al. (2006). Amazon rain forests green-up with sunlight in dry season. *Geophysical Research Letters*, 33, L06405, <http://dx.doi.org/10.1029/2005GL025583>.
- Jönsson, P., & Eklundh, L. (2002). Seasonality extraction by function fitting to time-series of satellite sensor data. *IEEE Transactions on Geoscience and Remote Sensing*, 40, 1824–1832.
- Justice, C. O., Vermote, E., Townshend, J. R. G., Defries, R., Roy, D. P., Hall, D. K., et al. (1998). The Moderate Resolution Imaging Spectroradiometer (MODIS): Land remote sensing for global change research. *IEEE Transactions on Geoscience and Remote Sensing*, 36, 1228–1249.
- Kaduk, J., & Heimann, M. (1996). A prognostic phenology scheme for global terrestrial carbon cycle models. *Climate Research*, 6, 1–19.
- La Mantia, T., Cullotta, S., & Garfi, G. (2003). Phenology and growth of *Quercus ilex* (L.) in different environmental conditions in Sicily (Italy). *Ecologia Mediterranea*, 29, 15–25.
- Ma, M., & Veroustraete, F. (2006). Reconstructing pathfinder AVHRR land NDVI time-series data for the Northwest of China. *Advances in Space Research*, 37, 835–840.
- McLachlan, G., & Peel, D. (2000). *Finite mixture models*. New York: John Wiley and Sons.
- Metzger, S., Junkermann, W., Mauder, M., Beyrich, F., Butterbach-Bahl, K., Schmid, H. P., et al. (2012). Eddy Covariance flux measurements with a weight-shift microlight aircraft. *Atmospheric Measurement Techniques*, 5, 2591–2643.
- Moulin, S., Kergoat, L., Viovy, N., & Dedieu, G. (1997). Global-scale assessment of vegetation phenology using NOAA-AVHRR satellite measurements. *Journal of Climate*, 10, 1154–1170.
- Nagler, P. L., Daughtry, C. S. T., & Goward, S. N. (2000). Plant litter and soil reflectance. *Remote Sensing of Environment*, 71, 207–215.
- Pontailler, J. -Y., & Genty, B. (1996). A simple red:far-red sensor using gallium arsenide phosphide detectors. *Functional Ecology*, 10, 535–540.

- Pontailleur, J. -Y., Hymus, G. J., & Drake, B. G. (2003). Estimation of leaf area index using ground-based remote sensed NDVI measurements: Validation and comparison with two indirect techniques. *Canadian Journal of Remote Sensing*, 29, 381–387.
- Reed, B. C., Brown, J. F., VanderZee, D., Loveland, T. R., Merchant, J. W., & Ohlen, D. O. (1994). Measuring phenological variability from satellite imagery. *Journal of Vegetation Science*, 5, 703–714.
- Saleska, S. R., Didan, K., Huete, A. R., & da Rocha, H. R. (2007). Amazon forests green-up during 2005 drought. *Science*, <http://dx.doi.org/10.1126/science.1146663>.
- Schwartz, M. D., Reed, B. C., & White, M. A. (2002). Assessing satellite-derived start-of-season measures in the conterminous USA. *International Journal of Climatology*, 22, 1793–1805.
- Sims, D. A., Rahman, A. F., Vermote, E. F., & Jiang, Z. (2011). Seasonal and inter-annual variation in view angle effects on MODIS vegetation indices at three forest sites. *Remote Sensing of Environment*, 115, 3112–3120.
- Sokal, R. R., & Michener, C. D. (1958). A statistical method for evaluating systematic relationships. *University of Kansas Scientific Bulletin*, 28, 1409–1438.
- Soudani, K., François, C., le Maire, G., Le Dantec, V., & Dufrêne, E. (2006). Comparative analysis of IKONOS, SPOT, and ETM+ data for leaf area index estimation in temperate coniferous and deciduous forest stands. *Remote Sensing of Environment*, 102, 161–175.
- Soudani, K., Hmimina, G., Delpierre, N., Pontailleur, J. -Y., Aubinet, M., Bonal, D., et al. (2012). Ground-based Network of NDVI measurements for tracking temporal dynamics of canopy structure and vegetation phenology in different biomes. *Remote Sensing of Environment*, 123, 234–245.
- Soudani, K., le Maire, G., Dufrêne, E., François, C., Delpierre, N., Ulrich, E., et al. (2008). Evaluation of the onset of green-up in temperate deciduous broadleaf forests derived from Moderate Resolution Imaging Spectroradiometer (MODIS) data. *Remote Sensing of Environment*, 112, 2643–2655.
- Studer, S., Stöckli, R., Appenzeller, C., & Vidale, P. (2007). A comparative study of satellite and ground-based phenology. *International Journal of Biometeorology*, 51, 405–414.
- Suzuki, R., Nomaki, T., & Yasunari, T. (2003). West–east contrast of phenology and climate in northern Asia revealed using a remotely sensed vegetation index. *International Journal of Biometeorology*, 47, 126–138.
- Tan, B., Woodcock, C. E., Hu, J., Zhang, P., Ozdogan, M., Huang, D., et al. (2006). The impact of gridding artifacts on the local spatial properties of MODIS data: Implications for validation, compositing, and band-to-band registration across resolutions. *Remote Sensing of Environment*, 105, 98–114.
- Van Leeuwen, W. J. D., & Huete, A. R. (1996). Effects of standing litter on the biophysical interpretation of plant canopies with spectral indices. *Remote Sensing of Environment*, 55, 123–138.
- Viovy, N., Arino, O., & Belward, A. S. (1992). The Best Index Slope Extraction (BISE): A method for reducing noise in NDVI time-series. *International Journal of Remote Sensing*, 13, 1585–1590.
- White, M. A., De Beurs, K. M., Didan, K., Inouye, D. W., Richardson, A. D., Jensen, O. P., et al. (2009). Intercomparison, interpretation, and assessment of spring phenology in North America estimated from remote sensing for 1982–2006. *Global Change Biology*, 15, 2335–2359.
- White, M. A., & Nemani, R. R. (2006). Real-time monitoring and short-term forecasting of land surface phenology. *Remote Sensing of Environment*, 104, 43–49.
- White, M. A., Nemani, R. R., Thornton, P. E., & Running, S. W. (2002). Satellite evidence of phenological differences between urbanized and rural areas of the Eastern United States deciduous broadleaf forest. *Ecosystems*, 5, 260–273.
- White, M. A., Thornton, P. E., & Running, S. W. (1997). A continental phenology model for monitoring vegetation responses to interannual climatic variability. *Global Biogeochemical Cycles*, 11, 217–234.
- Wolfe, R. E., Nishihama, M., Fleig, A. J., Kuyper, J. A., Roy, D. P., Storey, J. C., et al. (2002). Achieving sub-pixel geolocation accuracy in support of MODIS land science. *Remote Sensing of Environment*, 83, 31–49.
- Zhang, X., Friedl, M. A., Schaaf, C. B., Strahler, A. H., Hodges, J. C. F., Gao, F., et al. (2003). Monitoring vegetation phenology using MODIS. *Remote Sensing of Environment*, 84, 471–475.
- Zhang, X., & Goldberg, M. D. (2011). Monitoring fall foliage coloration dynamics using time-series satellite data. *Remote Sensing of Environment*, 115, 382–391.